Biochemical and Biophysical Research Communications 385 (2009) 84–87

Contents lists available at ScienceDirect

Biochemical and Biophysical Research Communications

journal homepage: www.elsevier.com/locate/ybbrc

Crystal structure of the *E. coli* tRNA^{Arg} aminoacyl stem isoacceptor RR-1660 at 2.0 Å resolution

André Eichert [a], Markus Perbandt [b], Dominik Oberthür [c], Angela Schreiber [a], Jens P. Fürste [a], Christian Betzel [c], Volker A. Erdmann [a], Charlotte Förster [a,*]

[a] Institute of Chemistry and Biochemistry, Free University Berlin, Thielallee 63, 14195 Berlin, Germany
[b] Institute of Biochemistry, Laboratory for Structural Biology of Infection and Inflammation, University of Lübeck, c/o DESY, Building 22a, 22603 Hamburg, Germany
[c] Institute of Biochemistry and Food Chemistry, University of Hamburg, Notkestr. 85, c/o DESY, Building 22a, 22603 Hamburg, Germany

ARTICLE INFO

Article history:
Received 21 April 2009
Available online 6 May 2009

Keywords:
tRNA identity elements
Acceptor stem microhelix
tRNA^{Arg}/Arg-tRNA-synthetase system
Crystal structure
RNA hydration pattern

ABSTRACT

Due to the redundancy of the genetic code there exist six mRNA codons for arginine and several tRNA^{Arg} isoacceptors which translate these triplets to protein within the context of the mRNA. The tRNA identity elements assure the correct aminoacylation of the tRNA with the cognate amino acid by the aminoacyl-tRNA-synthetases. In tRNA^{Arg}, the identity elements consist of the anticodon, parts of the D-loop and the discriminator base. The minor groove of the acceptor stem interacts with the arginyl-tRNA-synthetase. We crystallized different *Escherichia coli* tRNA^{Arg} acceptor stem helices and solved the structure of the tRNA^{Arg} isoacceptor RR-1660 microhelix by X-ray structure analysis. The acceptor stem helix crystallizes in the space group *P*1 with the cell constants $a = 26.28$, $b = 28.92$, $c = 29.00$ Å, $\alpha = 105.74$, $\beta = 99.01$, $\gamma = 97.44°$ and two molecules per asymmetric unit. The RNA hydration pattern consists of 88 bound water molecules. Additionally, one glycerol molecule is bound within the interface of the two RNA molecules.

Introduction

The aminoacylation of tRNAs with their cognate amino acids is assured by the correct interaction with the aminoacyl-tRNA-synthetases (aaRS). tRNA identity is governed by the tRNA determinants, which consist of different sequence and structure motifs. The tRNA/aaRS can be divided into two systems: Class I and class II [1]. Within Class I, the tRNA identity elements are relatively complex and consist of sequence- or structure motifs which are spread over different regions, mostly including the anticodon. In the Class II system, the aminoacyl-tRNA-synthetases depend on rather few and simple tRNA determinants, that are mainly located in the aminoacyl stem of the corresponding tRNAs and may even be so simple as to consist of only one single base pair [2].

The recognition between the aminoacyl-tRNA-synthetase and the tRNA is a crucial process to assure the accuracy in protein biosynthesis. Due to the redundancy of the genetic code and the existence of multiple mRNA codons for several amino acids, there often exist tRNA isoacceptors which have to be aminoacylated with the same amino acid. The arginine system is an example for the existence of multiple tRNA isoacceptors. The six arginine codons are accompanied by at least five tRNA^{Arg} isoacceptors in *Escherichia coli* [3]. The identity elements of tRNA^{Arg} and the arginyl-tRNA-synthetase structures are well investigated. The tRNA^{Arg}/Arginyl-tRNA synthetase belongs to the so-called 'Class I system' [1]. The tRNA^{Arg} identity elements consist of sequence motifs that are spread over different regions in the tRNA. They include the anticodon, the base at position 20 in the variable loop and the discriminator base at position 73 which is located prior to the conserved 3′CCA end of the tRNA [4–6]. The structure of the *Thermus thermophilus* ArgRS [6] and the complex between the yeast tRNA^{Arg} and the ArgRS [7,8] have been crystallized and the structures were solved by X-ray structure analysis showing new insights into the interaction between tRNA^{Arg} and ArgRS. The acceptor stem is not a carrier of identity elements in tRNA^{Arg}, but nevertheless, the minor groove of the tRNA^{Arg} aminoacyl stem interacts with the ArgRS.

We focus on comparative X-ray structure analysis of different tRNA acceptor stem microhelices. In the case of the tRNA^{Arg} system, the ArgRS has to assure the correct aminoacylation of at least five tRNA^{Arg} isoacceptors, which share the same identity elements but differ in sequence. The sequence of the tRNA^{Arg} aminoacyl stem varies to great extent within the isoacceptors. A structure comparison of different tRNA^{Arg} acceptor stem microhelices and following superposition experiments, like recently shown for the tRNA^{Gly} system [9], will help to further investigate this system. Additionally, docking experiments between the different tRNA^{Arg} acceptor stem microhelices and the synthetase will help to understand the tRNA^{Arg} acceptor stem–ArgRS binding in more detail, as has been done for the tRNA^{Ser} [10] system.

* Corresponding author. Fax: +49 30 838 56413.
E-mail address: foerster@chemie.fu-berlin.de (C. Förster).

0006-291X/$ - see front matter © 2009 Published by Elsevier Inc.
doi:10.1016/j.bbrc.2009.04.158

Also, the hydration pattern of RNA comes in the focus of interest, because the solvent plays an important role within the interacting surfaces between RNA and proteins. Due to an extensive hydration of the minor groove in RNA, governed by a specific hydration of the ribose 2′-OH group [11–13], the water contributes to the overall interaction between RNA and other macromolecules.

Here, we present the crystal structure of the *E. coli* $tRNA^{Arg}$ acceptor stem helix at 2.0 Å resolution. The RNA crystallizes in the space group *P*1 and the asymmetric unit consists of two microhelices, 88 bound water molecules and one glycerol molecule. The structure of the $tRNA^{Arg}$ acceptor stem helix, together with comparative studies of following $tRNA^{Arg}$ microhelix structures will contribute to a better understanding of the $tRNA^{Arg}$/ArgRS and the acceptor stem minor groove/synthetase interaction. Also, the structure will help to investigate the role of the extensive RNA hydration patterns.

Experimental procedures

Crystallization of the E. coli $tRNA^{Arg}$ isoacceptor RR-1660 microhelix. The sequence from the *E. coli* $tRNA^{Arg}$ acceptor stem microhelix, originating from the tRNA isoacceptor RR-1660, was derived from the tRNA data base [3]. The oligonucleotides 5′-$G_1C_2A_3U_4C_5C_6G_7$-3′ and 5′-$C_{66}G_{67}G_{68}A_{69}U_{70}G_{71}C_{72}$-3′ were annealed and crystallized according to Ref. [14]. Applying the hanging drop vapor diffusion technique, crystals appeared within 1 day at a temperature of 294 K with the following conditions: 0.5 M 2-(*N*-morpholino)ethanesulfonic acid (MES), pH 5.6, 10 mM magnesium chloride, 2.0 M lithium sulfate. The crystals, with approximate dimensions of $0.20 \times 0.05 \times 0.05$ mm, were flash-frozen in liquid nitrogen prior to data collection in the solution above containing additionally 20% (v/v) glycerol.

Acquisition of X-ray diffraction data. A data set was measured at the Elettra Synchrotron, Trieste, Italy, at the X-ray diffraction beam line XRD1 at a temperature of 100 K and a wavelength of 1.000 Å. The crystallographic data were collected from 50 to 1.70 Å and the data were processed within this range using the *HKL*-2000 package [15]. As merohedral disorder is known to occur in several small RNA helix crystals, the crystallographic data were analyzed for the possibility of merohedral twinning by applying the Padilla and Yeates algorithm [16], as implemented in the web server: http://nihserver.mbi.ucla.edu/pystats. The calculations gave the curve which corresponds to a theoretically untwinned crystal.

Structure determination and refinement. The structure of the *E. coli* $tRNA^{Arg}$ acceptor stem microhelix was solved with molecular replacement. A model was built using the human $tRNA^{Gly}$ aminoacyl stem microhelix (G9992; pdb ID: 2VUQ) [17], in which subsequently the bases were exchanged to the sequence of the *E. coli* $tRNA^{Arg}$ microhelix using the program *COOT* [18]. Molecular replacement calculations were applied using the program *PHASER* [19] as implemented in the *CCP4i* suite [20]. Structure refinement occurred by using the program *REFMAC5* [21] and the electron density maps were calculated by using *FFT* [22], all programs were used within the *CCP4i* suite [20]. The local geometric and the overall helical parameters of the $tRNA^{Arg}$ microhelix were calculated using the program *X3DNA* [23]. The coordinates of the *E. coli* $tRNA^{Arg}$ acceptor stem microhelix, isoacceptor RR-1660, have been deposited at the RCSB protein data bank with the pdb ID: 2W89.

Results and discussion

Crystallographic data and geometric parameters of the E. coli $tRNA^{Arg}$ microhelix

The sequence of the *E. coli* $tRNA^{Arg}$ acceptor stem microhelix with the data base ID: RR-1660 was derived from the tRNA data base [3] and consists of the two hybridized oligonucleotides 5′-$G_1C_2A_3U_4C_5C_6G_7$-3′ and 5′-$C_{66}G_{67}G_{68}A_{69}U_{70}G_{71}C_{72}$-3′ (Fig. 1). The microhelix crystallizes in the space group *P*1 with the cell constants: $a = 26.28$, $b = 28.92$, $c = 29.00$ Å, $\alpha = 105.74$, $\beta = 99.01$, $\gamma = 97.44°$ and two molecules per asymmetric unit [14] (Table 1). Molecular replacement calculations were used to solve the structure. The human $tRNA^{Gly}$ microhelix G9992 [17] served as an initial model, in which the sequence was subsequently changed and corrected to the sequence of the *E. coli* $tRNA^{Arg}$ microhelix. Crystallographic data were initially processed within a region of 40.0–1.70 Å and then refined to a resolution of 2.0 Å with *R*-values of $R/R_{free} = 21.1/25.5\%$ (Table 1). The asymmetric unit contains two RNA microhelices (Fig. 2) with 586 RNA atoms, 88 water molecules and one glycerol molecule. The glycerol is located within the interface between both $tRNA^{Arg}$ microhelices.

A selection of the average helical RNA parameters of the *E. coli* $tRNA^{Arg}$ microhelix and a comparison to other tRNA microhelices is shown in Table 2. The $tRNA^{Arg}$ acceptor stem shows the standard values as known for A-type RNA and reflects a typical RNA conformation without deviation from the idealized structure. All values describing the helical parameters like twist, rise, slide, roll, χ-displacement and propeller twist reflect the canonical A-RNA structure and lie in the region of the parameters shown for other tRNA microhelices (Table 2). No outliers can be detected in the single local helical parameters (data not shown). The phosphate backbone α/γ torsion angles adopt the (−) gauche/(+) gauche conformation. All β torsion angles show the anti conformation around ±180°. The sugar puckering is in the 2′-exo-conformation for all nucleotides, reflecting the typical A-RNA conformation (data not shown).

The RNA hydration pattern and ligands in the $tRNA^{Arg}$ microhelix structure

The $tRNA^{Arg}$ microhelix is surrounded by a detailed network of water molecules. We can detect 88 single solvent molecules which follow the general rules of RNA hydration. A detailed hydration picture of a selected base pair is shown in Fig. 3. Here, the U_{70}–

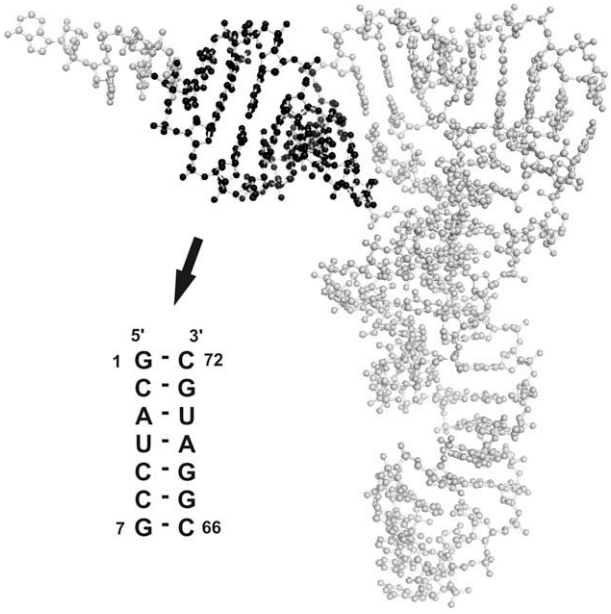

Fig. 1. The tRNA tertiary structure, demonstrated by using the yeast $tRNA^{Phe}$ [28]. The aminoacyl stem is highlighted in black and the sequence of the *E. coli* $tRNA^{Arg}$ acceptor stem microhelix, which structure was investigated here, is shown and pointed out by an arrow.

A_3 base pair is shown with a completely saturated solvent mask surrounding the nucleotides. Water molecules bind in the major and minor groove. The solvent molecules are in contact to the O4 of U_{70}, the exocyclic amino group and to the N7 of A_3 in the major groove. In the minor groove, the water molecules bind to the O2 of U_{70}, the 2′- hydroxyl group of the U_{70} ribose, the endocyclic N3 and to the 2′-hydroxyl group of A_3. These solvent molecules bridge to other water molecules which are associated in a solvent network,

Table 1
X-ray diffraction data and refinement statistics of the *E. coli* $tRNA^{Arg}$ acceptor stem microhelix isoacceptor RR-1660.

Space group	*P*1
Cell edges (Å)	$a = 26.28$, $b = 28.92$, $c = 29.00$
Cell angles (°)	$\alpha = 105.74$, $\beta = 99.01$, $\gamma = 97.44$
Radiation source	Elettra synchrotron, Trieste/beam line XRD1
Wavelength (Å)	1.000
Resolution range (Å)	40.0–1.70
No. of total reflections	12,812
No. of unique observations	7118
Completeness (%)	97.9 (93.2)
Multiplicity[a]	1.8 (1.7)
Average $I/\sigma(I)$[a,b]	22.2 (1.9)
R_{merge}[a,c] (%)	3.8 (16.5)
Molecules per asymmetric unit	2
Final R/R_{free} (%)[d]	21.1/25.5
RNA atoms	586
Glycerol molecules	1
Water oxygen atom loci	88
Rmsd bond lenghts (Å)[e]	0.019
Rmsd angles (°)[e]	2.55

[a] Values for the resolution shell 40–1.70 Å and in parenthesis for the highest resolution shell 1.73–1.70 Å.
[b] Reflection intensity.
[c] $R_{merge} = \sum_{hkl} \sum_i |I_i(hkl) - \langle I(hkl)\rangle| / \sum_{hkl} \sum_i I_i(hkl)$, where $I_i(hkl)$ and $\langle I(hkl)\rangle$ are the observed individual and mean intensities of a reflection with the indices *hkl*, respectively, $\sum_i$ is the sum over the individual measurements of a reflection with the indices *hkl*, and $\sum_{hkl}$ is the sum over all reflections.
[d] R_{free} = based on 5% of the data selected with [21].
[e] rmsd: root-mean-square deviation.

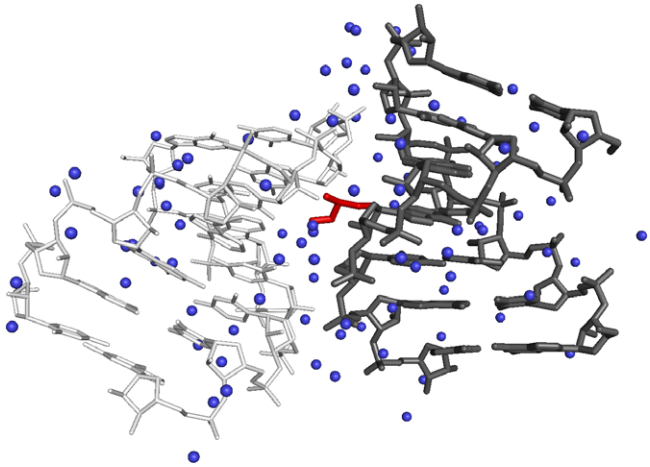

Fig. 2. The two *E. coli* $tRNA^{Arg}$ microhelices per asymmetric unit (shown in light and dark gray) surrounded by 88 solvent molecules (blue dots). A glycerol is bound in the interface between the two RNAs (red sticks). (For interpretation of color mentioned in this figure the reader is referred to the web version of the article.)

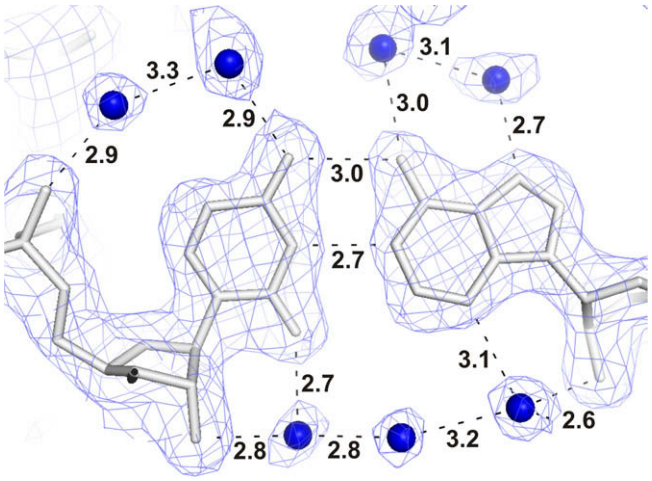

Fig. 3. The hydration network of the $tRNA^{Arg}$ microhelix as presented for the base pair U_{70}–A_3: 2*Fo–Fc* electron density map at 2.0 Å resolution with the nucleobases U_{70} and A_3 (gray sticks) and water molecules (blue balls). H-bond distances are shown by dashed lines and distances in Å are pointed out by numbers. (For interpretation of color mentioned in this figure the reader is referred to the web version of the article.)

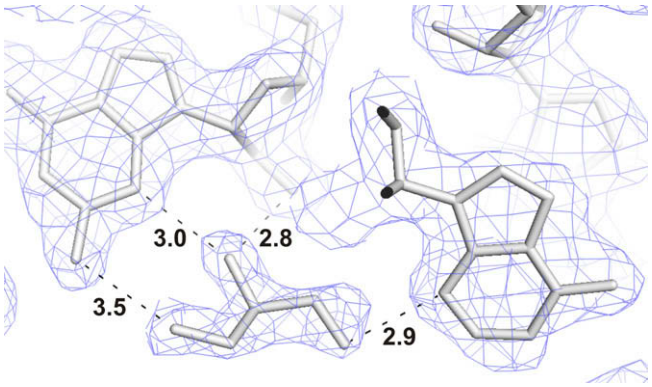

Fig. 4. The glycerol molecule bound in the interface between the two $tRNA^{Arg}$ microhelices. H-bonding occurs between the hydroxyl groups of the glycerol and the endocyclic N3, the exocyclic NH_2 group and 2′-OH group of G_{71} (first RNA, on the left) and to the N3 of A_{69} (second RNA, on the right). The 2*Fo–Fc* electron density map at 2.0 Å resolution is shown in blue. (For interpretation of color mentioned in this figure the reader is referred to the web version of the article.)

Table 2
Average helical parameters of the *E. coli* $tRNA^{Arg}$ microhelices (molecule A and B from the asymmetric unit) in comparison to the *E. coli* $tRNA^{Gly}$ (molecules A and B) [24], *E. coli* $tRNA^{Ser}$ microhelix [25], *E. coli* $tRNA^{Ala}$ microhelix [26,27] and to the generated yeast $tRNA^{Phe}$ microhelix, which was derived from Ref. [28].

	Twist (°)	Rise (Å)	Slide (Å)	Roll (°)	χ displacement (Å)	Prop. (°)
$tRNA^{Arg}$ microhelix A	32.37 ± 1.04	2.73 ± 0.16	−1.51 ± 0.24	5.85 ± 4.11	−3.69 ± 0.96	−8.23 ± 4.21
$tRNA^{Arg}$ microhelix B	32.05 ± 1.75	2.89 ± 0.13	−1.35 ± 0.26	7.44 ± 1.71	−3.60 ± 0.92	−12.27 ± 6.50
$tRNA^{Gly}$ microhelix A	30.95 ± 5.41	2.51 ± 0.15	−1.83 ± 0.11	7.49 ± 3.63	−4.72 ± 1.21	−9.81 ± 2.57
$tRNA^{Gly}$ microhelix B	31.26 ± 3.65	2.69 ± 0.20	−1.75 ± 0.51	7.64 ± 3.61	−4.34 ± 0.91	−8.85 ± 5.11
$tRNA^{Ser}$ microhelix	31.88 ± 3.78	2.71 ± 0.17	−1.62 ± 0.33	6.56 ± 2.25	−4.07 ± 1.36	−9.72 ± 4.55
$tRNA^{Ala}$ microhelix A	32.52 ± 3.50	2.57 ± 0.15	−1.59 ± 0.20	7.38 ± 1.58	−3.98 ± 0.80	−9.02 ± 3.19
$tRNA^{Ala}$ microhelix B	31.41 ± 2.78	2.68 ± 0.13	−1.56 ± 0.30	7.51 ± 3.52	−4.06 ± 1.21	−10.22 ± 4.81
generated $tRNA^{Phe}$ microhelix	32.54 ± 7.23	2.67 ± 0.24	−1.47 ± 0.24	8.42 ± 1.46	−3.97 ± 1.05	−12.17 ± 6.73

either contacting a second hydration layer or are in contact to the phosphate backbone of the RNA. This hydration network is of importance regarding tRNA–protein interactions. It will be of interest to perform superposition experiments to the Arginyl-tRNA-synthetase to investigate the role of the water molecules within the surface between both macromolecules. Also, the comparative structure analysis with other $tRNA^{Arg}$ microhelices will help to understand the $tRNA^{Arg}$ acceptor stem minor groove – ArgRS interaction in more detail.

A glycerol is located in the interface between the two $tRNA^{Arg}$ microhelices. The presence of glycerol in the structure can be explained by the addition of glycerol to the cryo-protecting buffer in which the RNA crystal was soaked prior to data collection. The interaction between the glycerol and the $tRNA^{Arg}$ microhelices can be described as following (Fig. 4): The first hydroxyl group of the glycerol binds to the endocyclic N3 of A_{69} from the first RNA molecule, whereas the second hydroxyl group contacts the endocyclic N3 and the 2′-OH group of G_{71} from the second RNA helix. The third hydroxyl group is in direct contact to a water molecule (not shown) and to the exocyclic amino group of G_{71} (Fig. 4). The glycerol acts like a bridging point between the two RNA molecules and possibly, this is the reason why its position is fixed in the structure. It is not of biological relevance, as it is part of the cryo-protecting conditions used during data acquisition. Nevertheless, within this region, the glycerol certainly displaces specific solvent molecules, since the minor groove of the RNA possesses the extensive hydration.

Further studies comprising comparative analysis to other $tRNA^{Arg}$ microhelix isoacceptors are underway. These investigations will contribute to further understanding of the $tRNA^{Arg}$–ArgRS interactions and to become insight into the role of tRNA hydration networks and the specific role of water molecules surrounding the tRNAs.

Acknowledgments

This work was supported within the RiNA network for RNA technologies by the Federal Ministry of Education and Research, the City of Berlin, and the European Regional Development Fund. We thank the Fonds der Chemischen Industrie (Verband der Chemischen Industrie e.V.) and the BMBF/VDI financed BiGRUDI network of the Robert Koch Institute (Berlin) for additional support. We gratefully acknowledge the DESY synchrotron (Hamburg, Germany) and the Elettra Synchrotron (Trieste, Italy) for providing beam time.

References

[1] G. Eriani, M. Delarue, O. Poch, J. Gangloff, D. Moras, Partition of tRNA synthetases into two classes based on mutually exclusive sets of sequence motifs, Nature 347 (1990) 203–206.
[2] Y.M. Hou, P. Schimmel, A simple structural feature is a major determinant of the identity of a transfer RNA, Nature 333 (1988) 140–145.
[3] M. Sprinzl, K.S. Vassilenko, Compilation of tRNA sequences and sequences of tRNA genes, Nucleic Acids Res. 33 (2005) D139–D140.
[4] W.H. McClain, K. Foss, R.A. Jenkins, J. Schneider, Nucleotides that determine Escherichia coli $tRNA^{Arg}$ and $tRNA^{Lys}$ acceptor identities revealed by analyses of mutant opal and amber suppressor tRNAs, Proc. Natl. Acad. Sci. USA 87 (1990) 9260–9264.
[5] L.H. Schulmann, H. Pelka, The anticodon contains a major element of the identity of arginine transfer RNAs, Science 246 (1989) 1595–1597.
[6] A. Shimada, O. Nureki, M. Goto, S. Takahashi, S. Yokoyama, Structural and mutational studies of the recognition of the arginine tRNA-specific major identity element, A20, by arginyl-tRNA synthetase, Proc. Natl. Acad. Sci. USA 98 (2001) 13537–13542.
[7] B. Delagoutte, D. Moras, J. Cavarelli, TRNA aminoacylation by arginyl-tRNA synthetase: induced conformations during substrates binding, EMBO J. 19 (2000) 5599–5610.
[8] B. Delagoutte, G. Keith, D. Moras, J. Cavarelli, Crystallization and preliminary X-ray crystallographic analysis of yeast arginyl-tRNA synthetase-yeast $tRNA^{Arg}$ complexes, Acta Crystallogr. D Biol. Crystallogr. 56 (2000) 492–494.
[9] C. Förster, A. Zerressen-Harte, J.P. Fürste, M. Perbandt, C. Betzel, V.A. Erdmann, Comparative X-ray structure analysis of human and *Escherichia coli* $tRNA^{Gly}$ acceptor stem microhelices, Biochem. Biophys. Res. Commun. 368 (2008) 1002–1006.
[10] C. Förster, A.B. Brauer, J.P. Fürste, C. Betzel, M. Weber, F. Cordes, V.A. Erdmann, Superposition of a $tRNA^{Ser}$ acceptor stem microhelix into the seryl-tRNA synthetase complex, Biochem. Biophys. Res. Commun. 362 (2007) 415–418.
[11] P. Auffinger, E. Westhof, Hydration of RNA base pairs, J. Biomol. Struct. Dyn. 16 (1998) 693–707.
[12] D.E. Draper, Themes in RNA–protein recognition, J. Mol. Biol. 293 (1999) 255–270.
[13] M. Sundaralingam, B. Pan, Hydrogen and hydration of DNA and RNA oligonucleotides, Biophys. Chem. 95 (2002) 273–282.
[14] A. Eichert, A. Schreiber, J.P. Fürste, M. Perbandt, C. Betzel, V.A. Erdmann, C. Förster, *Escherichia coli* $tRNA^{Arg}$ acceptor-stem isoacceptors: comparative crystallization and preliminary X-ray diffraction analysis, Acta Crystallogr. Sect. F Struct. Biol. Cryst. Commun. 65 (2009) 98–101.
[15] Z. Otwinowski, W. Minor, Processing of X-ray diffraction data collected in oscillation mode, Methods Enzymol. Macromol. Crystallogr. A 276 (1997) 307.
[16] J.E. Padilla, T.O. Yeates, A statistic for local intensity differences: robustness to anisotropy and pseudo-centering and utility for detecting twinning, Acta Crystallogr. D Biol. Crystallogr. 59 (2003) 1124–1130.
[17] C. Förster, M. Mankowska, J.P. Fürste, M. Perbandt, C. Betzel, V.A. Erdmann, Crystal structure of a human $tRNA^{Gly}$ microhelix at 1.2 A resolution, Biochem. Biophys. Res. Commun. 368 (2008) 996–1001.
[18] P. Emsley, K. Cowtan, Coot: model-building tools for molecular graphics, Acta Crystallogr. D Biol. Crystallogr. 60 (2004) 2126–2132.
[19] A.J. McCoy, R.W. Grosse-Kunstleve, L.C. Storoni, R.J. Read, Likelihood-enhanced fast translation functions, Acta Crystallogr. D Biol. Crystallogr. 61 (2005) 458–464.
[20] Collaborative Computational Project, Number 4, "The CCP4 Suite: Programs for Protein Crystallography", Acta Crystallogr. D 50 (1994) 760–763.
[21] G.N. Murshudov, A.A. Vagin, E.J. Dodson, Refinement of macromolecular structures by the maximum-likelihood method, Acta Crystallogr. D Biol. Crystallogr. 53 (1997) 240–255.
[22] R.J. Read, A.J. Schierbeek, A phased translation function, J. Appl. Cryst. 21 (1988) 490–495.
[23] X.J. Lu, W.K. Olson, 3DNA: a software package for the analysis, rRebuilding and visualization of three-dimensional nucleic acid structures, Nucleic Acids Res. 31 (2003) 5108–5121.
[24] C. Förster, A.B. Brauer, M. Perbandt, D. Lehmann, J.P. Fürste, C. Betzel, V.A. Erdmann, Crystal structure of an Escherichia coli $tRNA^{Gly}$ microhelix at 2.0 A resolution, Biochem. Biophys. Res. Commun. 363 (2007) 621–625.
[25] C. Förster, A.B. Brauer, S. Brode, J.P. Fürste, C. Betzel, V.A. Erdmann, $TRNA^{Ser}$ acceptor stem: conformation and hydration of a microhelix in a crystal structure at 1.8 A resolution, Acta Crystallogr. D Biol. Crystallogr. 63 (2007) 1154–1161.
[26] U. Mueller, Y.A. Muller, R. Herbst-Irmer, M. Sprinzl, U. Heinemann, Disorder and twin refinement of RNA heptamer double helices, Acta Crystallogr. D Biol. Crystallogr. 55 (1999) 1405–1413.
[27] U. Mueller, H. Schubel, M. Sprinzl, U. Heinemann, Crystal structure of acceptor stem of $tRNA^{Ala}$ from *Escherichia coli* shows unique G.U wobble base pair at 1.16 A resolution, RNA 5 (1999) 670–677.
[28] H. Shi, P.B. Moore, The crystal structure of yeast phenylalanine tRNA at 1.93 A resolution: a classic structure revisited, RNA 6 (2000) 1091–1105.